Chapter 2

Spark Plasma Sintering of Negative Temperature Coefficient Thermistor Ceramics

Aimin Chang, Bo Zhang, Yiquan Wu, Qing Zhao, Huimin Zhang, Jincheng Yao, Jinbao Xu and Pengjun Zhao

Additional information is available at the end of the chapter

http://dx.doi.org/10.5772/58496

1. Introduction

Spark plasma sintering (SPS), also known as field assisted sintering technique (FAST), belongs to a class of sintering techniques in which densification is enhanced by the simultaneous application of axial pressure and elevated temperature generated by a high current flow [1, 2]. SPS has been successfully used in the preparation of functionally graded materials [3], ceramics [4-6], magnetic materials [7, 8], alloy [9], etc. It is believed that the SPS has a significant advantages in decreasing the sintering temperature and sintering periods, and also preparing high density ceramics [10]. Although SPS has been widely used to prepare dense transparent and structural ceramics, little reports focus on the application of this technique to prepare dense ceramics for negative temperature coefficient (NTC) thermistor applications [11,12]. So this chapter first provides a summary of fundamental theoretical aspects of spark plasma sintering, and then the application of spark plasma sintering in NTC thermistor ceramics are introduced emphatically. At the end, the future research and application of spark plasma sintering in the NTC thermistor ceramics are forecasted.

2. Theoretical aspects of spark plasma sintering

SPS is a novel effective sintering technique, which has been used in the research and development of various kinds of materials. However, there is no uniform understanding in the sintering mechanism of SPS. In general, SPS is a pressure sintering method based on the simultaneous application of axial pressure and high temperature plasma momentarily generated in the gaps between powder materials by electrical discharge at the beginning of ON-OFF DC pulse energizing [13]. In addition to have the Joule heating due to the electric current and plastic deformation produced by pressure, SPS also generates DC pulse voltage between the powder particles, and effectively makes use of the spontaneous heat generated by the discharge between powder particles, thus resulting in some special characteristics. Compared to the conventional sintering, SPS has two important characteristics [14, 15]: (1) SPS process can make high-energy pulse focus on the grain junction point, thus saving the energy; (2) A high energy, low voltage spark pulse current momentarily generates spark plasma and produces a high localized temperature from several to ten thousand °C between the particles and then resulting in optimum thermal diffusion and grain boundary migration, i.e. more material transfer can be intensified and thus high density ceramics can be obtained through spark plasma sintering with a low sintering temperature and a short sintering period. Fig. 1 shows the schematic of SPS furnace [16].

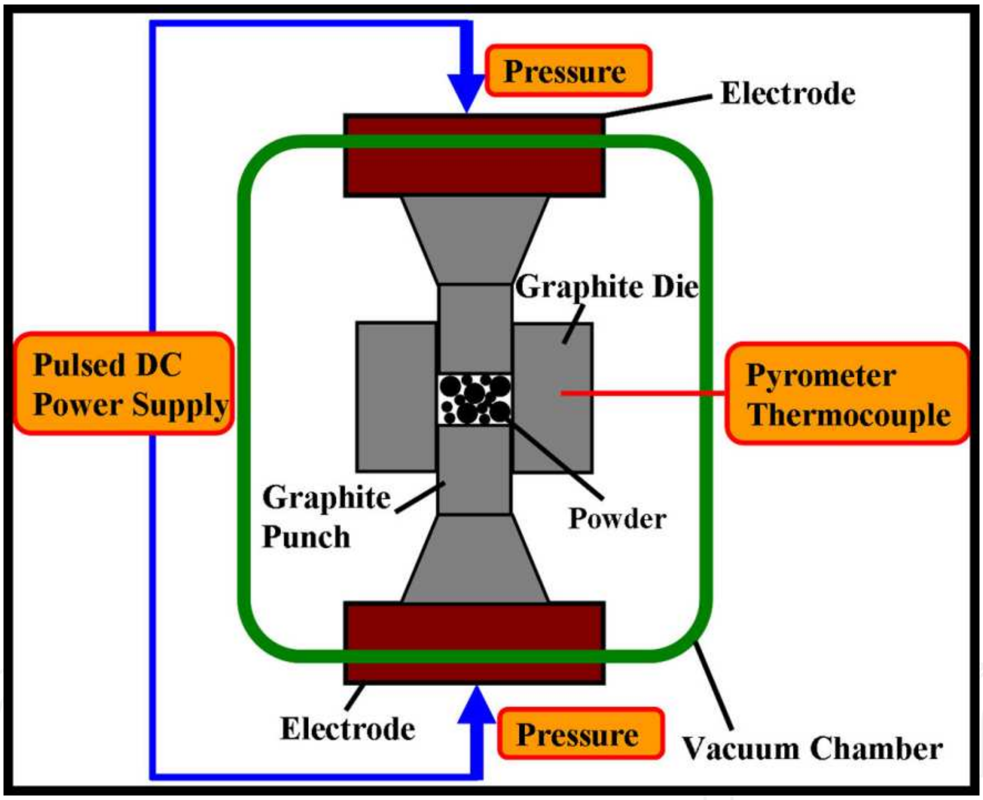

Figure 1. Schematic of SPS furnace [16].

3. Application of spark plasma sintering in NTC thermistor ceramics

In the past decades, more advanced techniques such as microwave sintering [17, 18], and nitrogen atmosphere sintering [19] have been used for NTC ceramic powder consolidation. However, there are few reports focusing on the application of SPS technique to prepare dense ceramics for NTC thermistor applications. The advantages of spark plasma sintering against conventional sintering for high temperature NTC thermistor ceramics are reviewed as follows.

3.1. Brief introduction of NTC thermistors

NTC thermistors are thermally sensitive resistors whose resistance decreases with increasing temperature. Their resistivity can be expressed by the following Arrhenius equation [20, 21]: $\rho=\rho_o\exp(Ea/kT)$, where ρ_o is the resistivity of the material at infinite temperature, T is the absolute temperature, Ea is the activation energy for electrical conduction, and k is the Boltzmann constant. They are mainly used in industrial areas as elements for temperature measurements, control, etc [22].

In the past few years, development of novel high temperature NTC thermistor materials has been motivated by the requirements of particle filters and catalytic converters in exhaust pipe for automotive motors [23, 24]. NTC thermistor ceramics composed of spinel structure (MMn_2O_4, where M=Ni, Co, Fe, Cu, Zn) show aging of the electrical properties and their application is commonly limited to temperatures below 300°C [25, 26]. The literature suggests that rare earth (Sm, Tb, Y, etc) perovskite oxides (ABO_3) can be used for measurements from ambient to 1000°C [23]. In particular, $YCrO_3$ having an orthorhombic perovskite structure, has been considered as a candidate for high temperature NTC thermistor applications [19, 23, 27, 28]. However, the material shows poor sinterability and is difficult to densify under ambient atmospheric conditions or through pressureless sintering techniques [29, 30]. We have investigated the spark plasma sintering of $YCr_{1-x}Mn_xO_3$ ceramics and $MgAl_2O_4$-$YCr_{0.5}Mn_{0.5}O_3$ composite ceramics, and their NTC electrical properties.

3.2. Spark plasma sintering and electrical properties of $YCr_{1-x}Mn_xO_3$ NTC ceramics

In the conventional sintering processes, extremely high sintering temperatures (up to 1600°C) and long holding time (several hours) in air are applied in the fabrication of $YCrO_3$ ceramics to achieve the highest density and minimum porosity. The poor sinterability of $YCrO_3$ material is attributed to the loss of Cr_2O_3 through its volatility during sintering process [30, 31]. In our previous work [32, 33], $YCr_{1-x}Mn_xO_3$ ($0\leq x\leq 0.5$) NTC ceramics with a high relative density have been obtained by combing the Pechini method synthesis and SPS. Fig.2 shows the flow chart for the fabrication of $YCr_{1-x}Mn_xO_3$ thermistor powders by a Pechini method. The molar ratio of citric acid, ethylene glycol and metal ions was 1.5:1.5:1. The spark plasma sintering was carried out in vacuum (6 Pa) with an apparatus (FCT Systeme GmbH, FCT, Rauenstein, Germany). The SPS equipment used in the experiments is shown in Fig. 3. Fig.4 shows the time dependence of the temperature and applied pressure during SPS process. The sintering temperature was 1300 ∘C, and the dwell time was 10 min. Fig.5 shows the XRD patterns of the SPS-sintered $YCr_{1-x}Mn_xO_3$ ceramics. All samples had a pure orthorhombic perovskite phase isomorphic to $YCrO_3$ (JCPDF 34-0365) described by the space group *Pnma*, and no secondary phase occurred with the increase of Mn concentration. Fig.6 shows the SEM images of surface section of SPS-sintered $YCr_{1-x}Mn_xO_3$ ceramics. It can be seen that as-sintered $YCrO_3$ ceramics were highly dense, and had a bulk density of 5.6112 g/cm^3, corresponding to 97.6% of the theoretical density (5.751 g/cm^3) [33]. One can observe that grain size decreased with the increase of Mn content. This result may be due to the dragging effect between Mn ions and grain boundary, which increases the energy for the movement of grain boundary and retards the grain growth [34, 35]. The $YCr_{1-x}Mn_xO_3$ NTC thermistor over a wide temperature range of 25 to 300 °C showed a linear relationship between the logarithm of the resistivity and the reciprocal of the absolute temperature. And the resistivity increased at first and then decreased with increasing Mn contents, which had the same varying tendency with activation energy. This electrical conductivity anomaly has been revealed by using defect chemistry theory combination with X-ray photoelectron spectroscopy analysis [32]: The major carriers in $YCrO_3$ are holes. Mn ions are acting as an n-type dope, and partly compensate for the effect of metal vacancies, thus leading to an increase in the resistivity. Mn^{4+} ions increase as Mn content increases from 0.2 to 0.5, which promote the rise in charge carriers and the electron hopping, thereby resulting in a decrease in the resistivity. Therefore, SPS has shown significant advantages against conventional sintering in the fabrication of high density $YCr_{1-x}Mn_xO_3$ ceramics, and provides efficient and viable means for the study of the conduction mechanism of NTC thermistors.

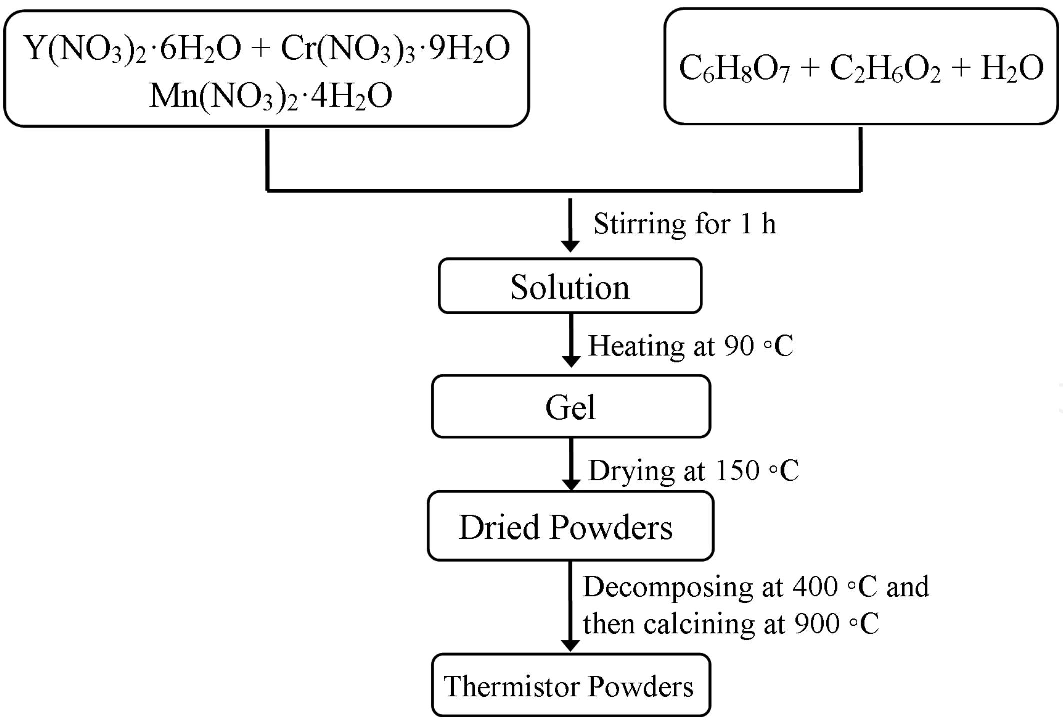

Figure 2. Flow chart for the fabrication of $YCr_{1-x}Mn_xO_3$ thermistor powders by a Pechini method.

Figure 3. Image of SPS equipment (From Alfred University).

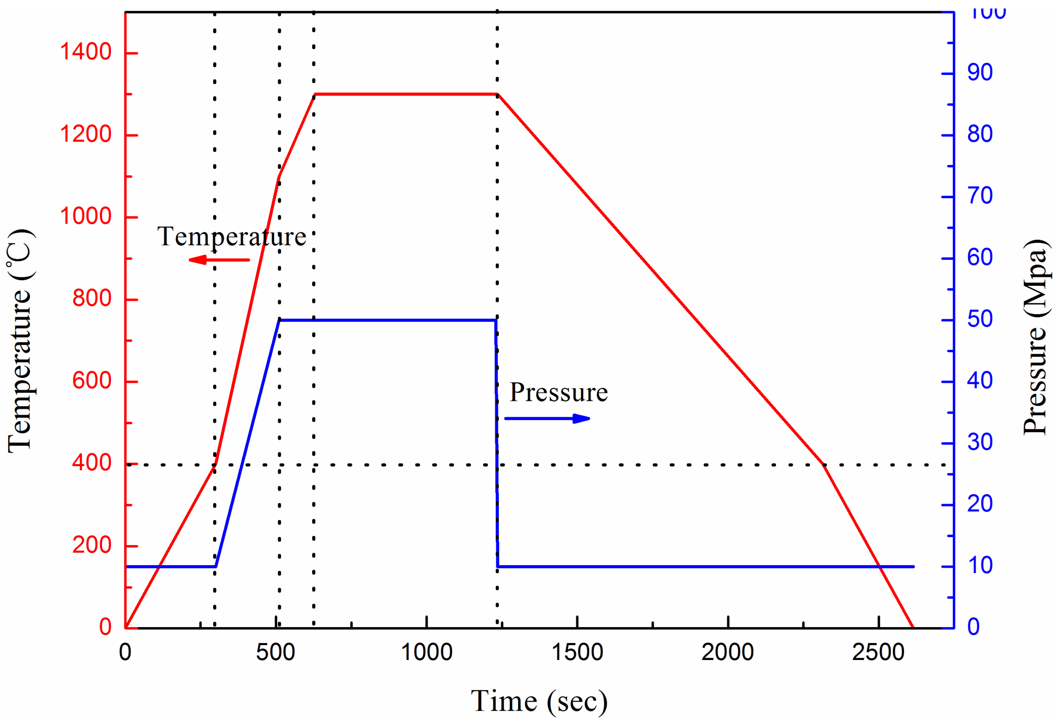

Figure 4. Time dependence of the temperature and applied pressure during SPS process [33].

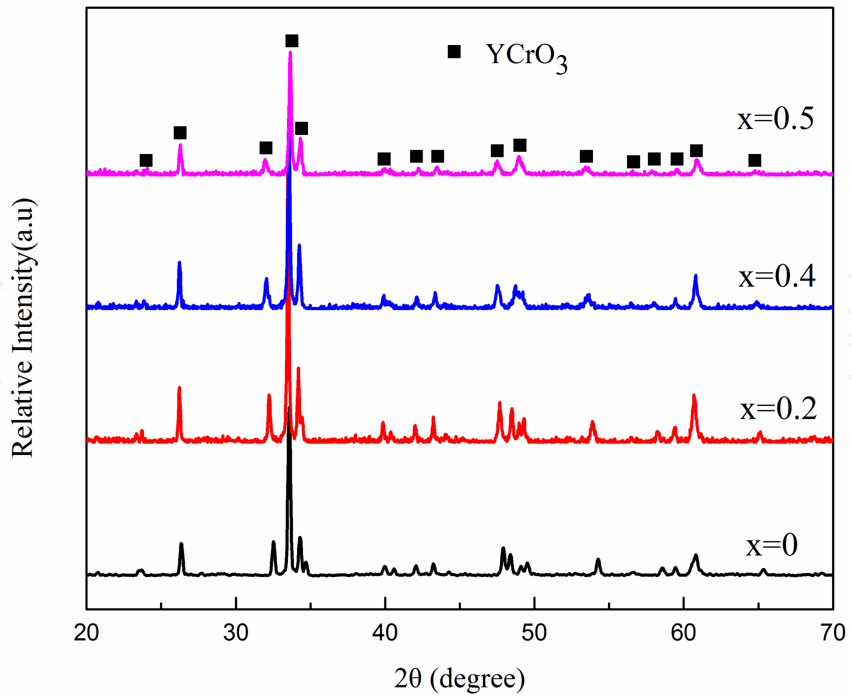

Figure 5. XRD patterns of the SPS-sintered $YCr_{1-x}Mn_xO_3$ ceramics [32].

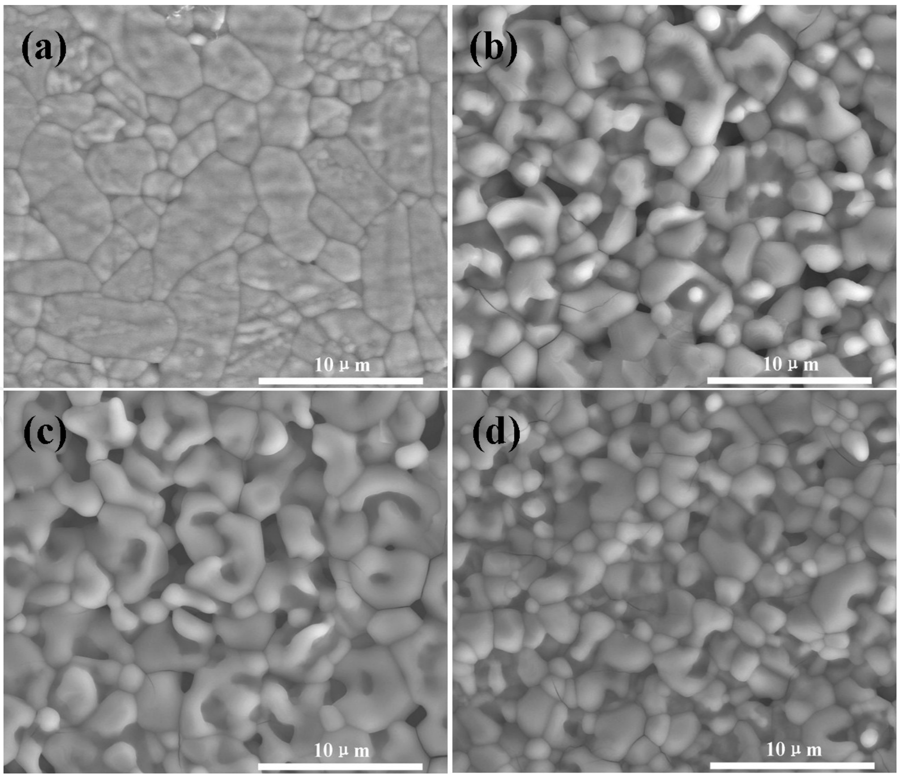

Figure 6. SEM images of surface section of SPS-sintered $YCr_{1-x}Mn_xO_3$ ceramics: (a) x=0; (b) x=0.2; (c) x=0.4; (d) x=0.5.

3.3. Spark plasma sintering and electrical properties of $MgAl_2O_4$-$YCr_{0.5}Mn_{0.5}O_3$ composite NTC ceramics

Recently, there is an increasing interest in exploring NTC behavior in composite materials because of their high temperature potential for combining properties that are difficult to attain separately with the individual component [24]. We have designed and prepared $x$$MgAl_2O_4$-(1-$x$)$YCr_{0.5}Mn_{0.5}O_3$ high temperature composite thermistor ceramics by associating a less resistive phase $YCr_{0.5}Mn_{0.5}O_3$ with a high resistive $MgAl_2O_4$ combination with spark plasma sintering [12]. Fig.7 shows the time dependence of the temperature and applied pressure during SPS process. The sintering temperature was 1200∘C, and the dwell time was 20 min. The SPS-sintered composite ceramics consisted of a cubic spinel $MgAl_2O_4$ phase and an orthorhombic perovskite $YCr_{0.5}Mn_{0.5}O_3$ phase isomorphic to $YCrO_3$. Fig. 8 exhibits the micro-structures of the SPS-sintered samples. The SPS-sintered ceramics were highly dense, and their grain sizes were ranging from 0.5 to 2 μm. The relative densities were 95.5%, 97.4% and 94.1% of the theoretical density for x=0.1, 0.4, 0.6, respectively. The resistivity of composite ceramics decreased with increasing temperature from 25 to 1000 ∘C, indicative of NTC characteristics. The obtained ρ_{25}, $B_{25\text{-}150}$, $B_{700\text{-}1000}$, $Ea_{25/150}$ and $Ea_{700/1000}$ of the SPS-sintered composite NTC thermistors were in the range of 1.53×10^6-9.92×10^9 Ωcm, 3380-5172 K, 7239-9543 K, 0.291~0.446 eV, 0.624~0.823 eV, respectively. This result indicates that these values can be adjusted by changing $MgAl_2O_4$ content. Fig. 9 compares the temperature dependence of electrical resis-tivity ρ of the samples $0.4MgAl_2O_4$-$0.6YCr_{0.5}Mn_{0.5}O_3$sintered by conventional sintering (CS) and SPS. It can be seen that the samples from SPS-sintered ceramics possessed a higher resistivity than that from conventional sintered ceramics. there are two possible reasons for the increase in the resistivity of SPS-sintered samples [12]: (1) During the SPS process, the short sintering period is advantageous in reducing chromium volatilization, thus leading to a decrease in Cr^{4+} and Mn^{4+} ion concentration, thereby increasing the resistivity as a result; (2) SPS-sintered

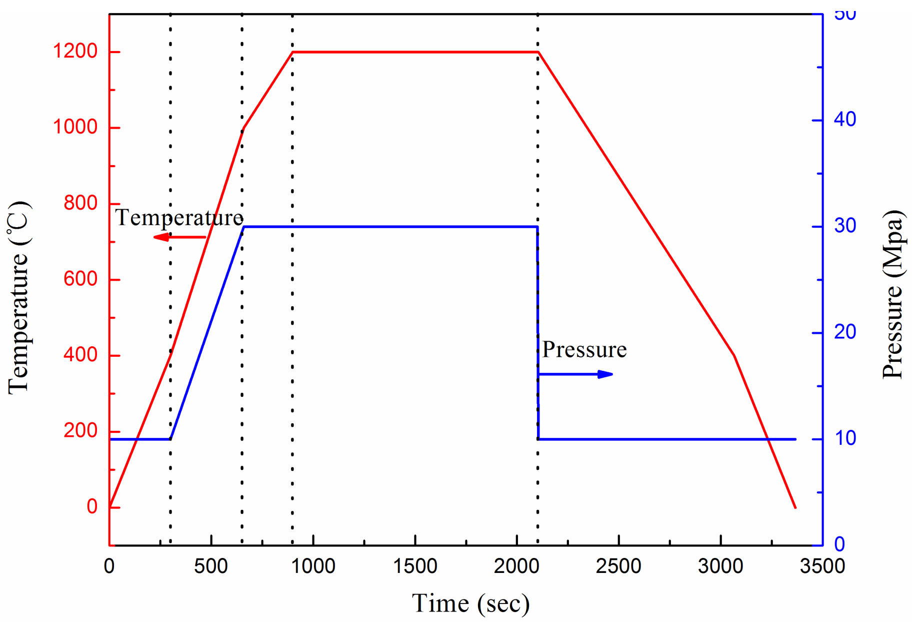

Figure 7. Time dependence of the temperature and applied pressure during SPS process.

samples have a smaller grain size, resulting in a decrease in the time between electron scattering events of charge carriers and thus increasing the resistivity [36]. In conclusion to this, SPS has potential superiority on synthesis high temperature NTC ceramic materials.

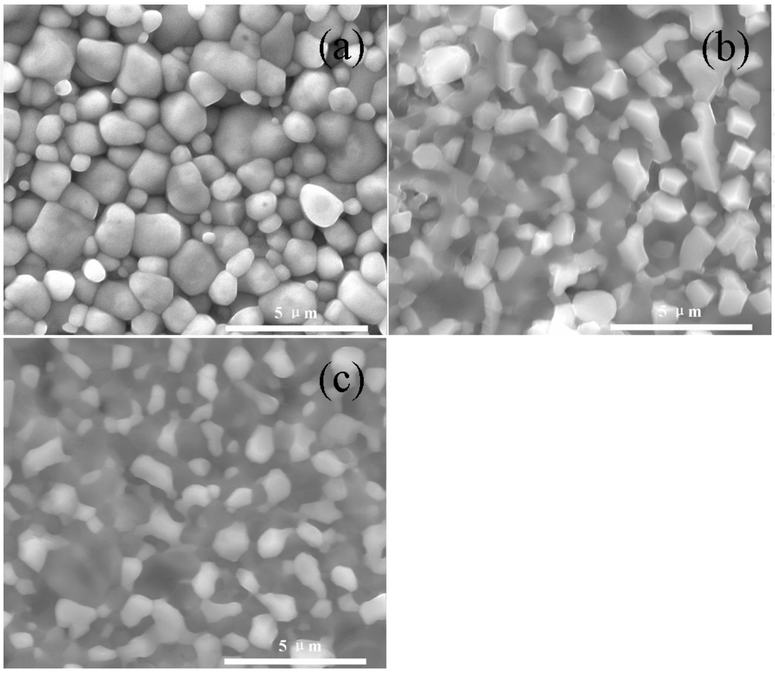

Figure 8. SEM images of the SPS-sintered xMgAl$_2$O$_4$-(1-x)YCr$_{0.5}$Mn$_{0.5}$O$_3$ composite ceramics: (a) x=0.1; (b) x=0.4; (c) x=0.6 [12].

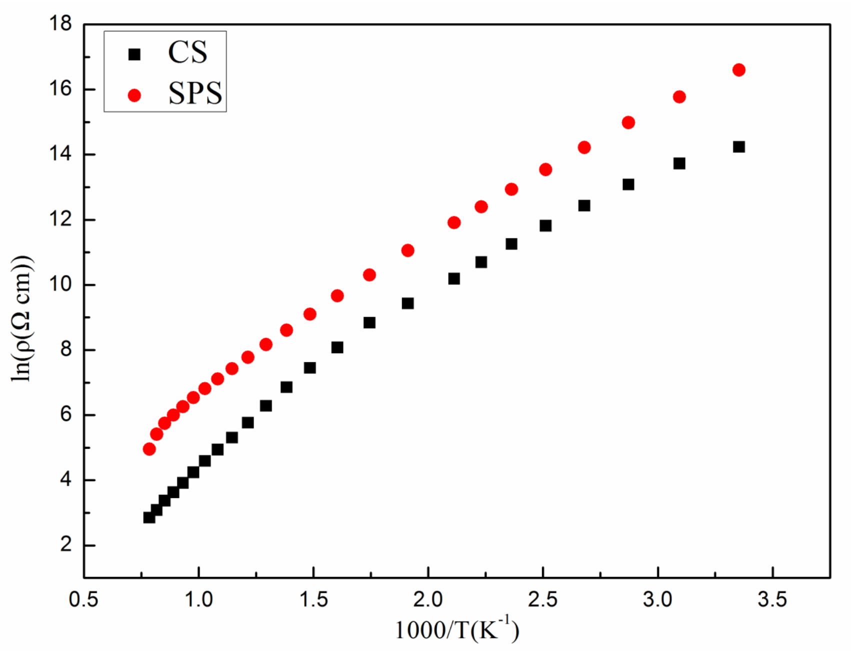

Figure 9. Temperature dependence of electrical resistivity ρ of the samples 0.4MgAl$_2$O$_4$-0.6YCr$_{0.5}$Mn$_{0.5}$O$_3$ sintered by conventional sintering (CS) and SPS [12].

4. Summary

The fundamentals, applications of spark plasma sintering to thermistor ceramics are reviewed in this chapter. For thermistor ceramics, the advantages of spark plasma sintering against traditional sintering are as follows: (1) Faster heating rate decreases the sintering time by using spark plasma sintering, and thus saving energy than traditional sintering; (2) Spark plasma sintering can ensure ceramics with high density and small grain at a low sintering temperature and a short sintering period. What's more, spark plasma sintering has shown significant advantages in the fabrication of $YCrO_3$ perovskite-based thermistor ceramics and provides an efficient mean for the study of the conduction mechanism of NTC thermistors.

In the past years, there have had a significant developments and advances regarding to the spark plasma sintering of ceramics. However, the fundamental theory of spark plasma sintering is not fully understood, and also needs massive fundamental research and practical innovation to perfect. It can be forecasted that there is a great future for the successful commercialization of spark plasma sintering in ceramic preparation.

Author details

Aimin Chang[1*], Bo Zhang[1], Yiquan Wu[3], Qing Zhao[1,2], Huimin Zhang[1], Jincheng Yao[1], Jinbao Xu[1] and Pengjun Zhao[1,2]

*Address all correspondence to: changam@ms.xjb.ac.cn

1 Key Laboratory of Functional Materials and Devices for Special Environments of CAS; Xinjiang Key Laboratory of Electronic Information Materials and Devices; Xinjiang Technical Institute of Physics & Chemistry of CAS, Urumqi, China

2 University of Chinese Academy of Sciences, Beijing, China

3 Kazuo Inamori School of Engineering, New York State College of Ceramics at Alfred University, Alfred, NY, USA

References

[1] S. Meir, S. Kalabukhov, N. Froumin, M.P. Dariel, N. Frage, Synthesis and densification of transparent magnesium aluminate spinel by SPS processing, Journal of the American Ceramic Society, 92 (2009) 358-364.

[2] K. Vanmeensel, A. Laptev, O. Van der Biest, J. Vleugels, Field assisted sintering of electro-conductive ZrO_2-based composites, Journal of the European Ceramic Society, 27 (2007) 979-985.

[3] R. Watanabe, T. Nishida, T. Hirai, Present status of research on design and processing of functionally graded materials, Metals and Materials International, 9 (2003) 513-519.

[4] N. Gao, J. Li, D. Zhang, Y. Miyamoto, Rapid synthesis of dense Ti_3SiC_2 by spark plasma sintering, Journal of the European Ceramic Society, 22 (2002) 2365-2370.

[5] J.G. Noudem, D. Kenfaui, S. Quetel-Weben, C.S. Sanmathi, R. Retoux, M. Gomina, Spark Plasma Sintering of n-Type Thermoelectric $Ca_{0.95}Sm_{0.05}MnO_3$, Journal of the American Ceramic Society, 94 (2011) 2608-2612.

[6] J.G. Noudem, A new process for lamellar texturing of thermoelectric $Ca_3Co_4O_9$ oxides by spark plasma sintering, Journal of the European Ceramic Society, 29 (2009) 2659-2663.

[7] J. Sun, G. Sun, W. Qu, Synthesis of dense NiZn ferrites by spark plasma sintering, Ceramics International, 28 (2002) 855–858.

[8] B.L. Shen, H. Kimura, A. Inoue, Fabrication of Fe-based glassy cores with high saturation magnetization and good soft magnetic properties by spark plasma sintering, Materials Science Forum, (2005) 3397-3400.

[9] W.S. Liu, B.P. Zhang, J.F. Li, H. L. Zhang, L. D. Zhao, Enhanced thermoelectric properties in CoSb3-xTex alloys prepared by mechanical alloying and spark plasma sintering, Journal of Applied Physics, 102 (2007) 103717.

[10] N. Frage, S. Cohen, S. Meir, S. Kalabukhov, M.P. Dariel, Spark plasma sintering (SPS) of transparent magnesium-aluminate spinel, Journal of Materials Science, 42 (2007) 3273-3275.

[11] T. Takeuchi, Y. Takeda, R. Funahashi, T. Aihara, M. Tabuchi, H. Kageyama, Rapid Preparation of Dense $(La_{0.9}Sr_{0.1})CrO_3$ Ceramics by Spark-Plasma Sintering, Journal of The Electrochemical Society, 147 (2000) 3979-3982.

[12] B. Zhang, Q. Zhao, A. Chang, Y. Li, Y. Liu, Y. Wu, Spark plasma sintering of $MgAl_2O_4$-$YCr_{0.5}Mn_{0.5}O_3$ composite NTC ceramics, Journal of the European Ceramic Society, 34 (2014) 2989-2995.

[13] M. Tokita, Mechanism of spark plasma sintering, in: Proceeding of NEDO International Symposium on Functionally Graded Materials, Japan, (1999) 22.

[14] L. Gao, H. Miyamoto, Spark plasma sintering technology, Journal of Inorganic Materials, 12 (1997) 129-133.

[15] M. Suárez, A. Fernández, J. Menéndez, R. Torrecillas, H. Kessel, J. Hennicke, R. Kirchner, T. Kessel, Challenges and Opportunities for Spark Plasma Sintering: A Key Technology for a New Generation of Materials, Intech-Open Access Publisher, (2013) 319-342.

[16] http://www.mfm.uni-jena.de/Forschung/FAST+_+SPS.html.

[17] X. Jin, A. Chang, H. Zhang, D. Zhang, Preparation and Microwave Sinterability of $Mn_{0.43}Ni_{0.9}CuFe_{0.67}O_4$ NTC Thermistor Materials by Pechini Method, Journal of Inorganic Materials, 24 (2009) 1013-1018.

[18] X. Jin, A. Chang, H. Zhang, D. Zhang, A Comparison Study of Sinterability and Electrical Properties for Microwave and Conventional Sintered $Mn_{0.43}Ni_{0.9}CuFe_{0.67}O_4$ Ceramics, Journal of Materials Science & Technology, 26 (2010) 344-350.

[19] A. Kamlo, J. Bernard, C. Lelievre, D. Houivet, Synthesis and NTC properties of $YCr_{1-x}Mn_xO_3$ ceramics sintered under nitrogen atmosphere, Journal of the European Ceramic Society, 31 (2011) 1457-1463.

[20] K. Park, J. Lee, The effect of ZnO content and sintering temperature on the electrical properties of Cu-containing $Mn_{1.95-x}Ni_{0.45}Co_{0.15}Cu_{0.45}Zn_xO_4$ ($0 \leq x \leq 0.3$) NTC thermistors, Journal of Alloys and Compounds, 475 (2009) 513-517.

[21] Y. Luo, X. Liu, G. Chen, Effect of Y_2O_3 addition on the electrical properties of $BaTiO_3$-based NTC thermistors, Materials Letters, 60 (2006) 1011-1013.

[22] K. Park, J. Lee, S.J. Kim, W.S. Seo, W.S. Cho, C.W. Lee, S. Nahm, The effect of Zn on the microstructure and electrical properties of $Mn_{1.17-x}Ni_{0.93}Co_{0.9}Zn_xO_4$ ($0 \leq x \leq 0.075$) NTC thermistors, Journal of Alloys and Compounds, 467 (2009) 310-316.

[23] D. Houivet, J. Bernard, J.M. Haussonne, High temperature NTC ceramic resistors (ambient-1000 ∘C), Journal of the European Ceramic Society, 24 (2004) 1237-1241.

[24] B. Zhang, Q. Zhao, A. Chang, H. Yan, Y. Wu, $MgAl_2O_4$-$LaCr_{0.5}Mn_{0.5}O_3$ composite ceramics for high temperature NTC thermistors, Journal of Materials Science: Materials in Electronics, 24 (2013) 4452-4456.

[25] M. Deepa, P.P. Rao, S. Sumi, A.N.P. Radhakrishnan, P. Koshy, New Negative Temperature Coefficient Ceramics in Ca-Ce-Nb-M-O (M=Mo or W) System, Journal of the American Ceramic Society, 93 (2010) 1576-1579.

[26] B. Zhang, Q. Zhao, A. Chang, J. Yao, P. Zhao, F. Guan, W. Kong, Complex impedance analysis of (Y_2O_3+CeO_2)–$YCr_{0.5}Mn_{0.5}O_3$ composite NTC ceramics, Journal of Alloys and Compounds, 512 (2012) 132-139.

[27] C. Nivot, J. Bernard, C. Lelievre, J.-M. Haussonne, D. Houivet, Moisture sensitivity of $YCr_{(1-x)}Mn_xO_3$ perovskites, Ceramics International, 36 (2010) 929-935.

[28] K. Fujiwara, S. Lee, N. Donnelly, T. Yamaguchi, C.A. Randall, Resistance Degradation in $Y(Cr,Mn)O_3$-Y_2O_3 Composite NTC Ceramics in Hostile Environments, Journal of the American Ceramic Society, 92 (2009) 2634-2641.

[29] T. Tachiwaki, Y. Kunifusa, M. Yoshinaka, K. Hirota, O. Yamaguchi, Formation, densification, and electrical conductivity of air-sinterable $Y(Cr_{1-x}Mg_x)O_3$ prepared by the hydrazine method, Materials Science and Engineering B, 86 (2001) 255-259.

[30] A. Durán, A. Arévalo-López, E. Castillo-Martínez, M. García-Guaderrama, E. Moran, M. Cruz, F. Fernández, M. Alario-Franco, Magneto-thermal and dielectric properties

of biferroic $YCrO_3$ prepared by combustion synthesis, Journal of Solid State Chemistry, 183 (2010) 1863-1871.

[31] T. Tachiwaki, Y. Kunifusa, M. Yoshinaka, K. Hirota, O. Yamaguchi, Formation, powder characterization and sintering of $YCrO_3$ prepared by a sol–gel technique using hydrazine, International Journal of Inorganic Materials, 3 (2001) 107-111.

[32] B. Zhang, Q. Zhao, A. Chang, Y. Li, Y. Liu, Y. Wu, Electrical conductivity anomaly and X-ray photoelectron spectroscopy investigation of $YCr_{1-x}Mn_xO_3$ negative temperature coefficient ceramics, Applied Physics Letters, 104 (2014) 102109.

[33] B. Zhang, Q. Zhao, A. Chang, Y. Liu, Y. Li, Y. Wu, Synthesis of $YCrO_3$ ceramics through a field-assisted sintering technique, Journal of Materials Science: Materials in Electronics, 25 (2014) 1400-1403.

[34] J. Yao, B. Zhang, J. Wang, A. Chang, G. Ji, P. Zhao, L. Zhao, Preparation of $Ni_{0.9}Mn_{2.1-x}Mg_xO_4$ ($0 \le x \le 0.3$) negative temperature coefficient ceramic materials by a rheological phase reaction method, Materials Letters, 112 (2013) 69-71.

[35] J. Wang, J. Zhang, Structural and electrical properties of $NiMg_xMn_{2-x}O_4$ NTC thermistors prepared by using sol-gel derived powders, Materials Science and Engineering: B, 176 (2011) 616-619.

[36] K. Park, Fabrication and Electrical Properties of Mn-Ni-Co-Cu-Si Oxides Negative Temperature Coefficient Thermistors, Journal of the American Ceramic Society, 88 (2005) 862-866.